CICE 2023 Rio de Janeiro – Brazil 11TH INTERNATIONAL CONFERENCE ON FRP COMPOSITES IN CIVIL ENGINEERING

ENHANCING MECHANICAL PROPERTIES OF TRM USING BIAXIAL PVA MESH AND SHCC

Gauri M. Kumbhojkar, Brunel University London, UK, gaurimahesh.kumbhojkar@brunel.ac.uk
Esmaeel Esmaeeli, Brunel University London, UK, esmaeel.esmaeeli@brunel.ac.uk
Omar B. Kasbah, Frankham Consultancy Group, UK, omar4732@gmail.com

ABSTRACT
This study explores the benefits of combining Strain Hardening Cementitious Composite (SHCC) with biaxial Polyvinyl Alcohol (PVA) mesh to develop TR-SHCC. The hydrophilic nature and modulus of elasticity of PVA foster a strong bond and efficient stress redistribution within the composite. Tensile testing of a PVA-SHCC reinforced with different layouts of a PVA textile grid revealed that a three double-layer (3DL) configuration significantly improves tensile strength and strain-hardening capacity over the baseline SHCC. It also maintains an average crack width below 150 µm at 4% strain-hardening, a promising feature for applications in corrosive environments subject to dynamic actions such as earthquakes.

KEYWORDS
Textile Reinforced Mortar (TRM); Strain hardening capacity; PVA textile grid; Tensile behaviour.

INTRODUCTION
Despite Fibre Reinforced Polymers (FRPs) being at the forefront of the solutions for strengthening and retrofitting masonry and reinforced concrete (RC) structures for several decades, the poor performance of their epoxy resin at elevated temperatures, incompatibility with substrate materials, and premature debonding, for example, restrict the scope of their application.

Hybrid Composite Plate (HCP), a relatively recent innovation, addresses most FRP's limitations. This prefabricated plate is composed of an ultra-ductile fibrous mortar, known as Strain Hardening Cementitious Composite (SHCC), which is further reinforced by externally bonded or near-surface mounted Carbon Fibre Reinforced Polymers (CFRP) (Esmaeeli et al., 2013; Esmaeeli, 2015). The SHCC is achieved by mixing an appropriate type and volume of short, dispersed fibres into a finely graded cementitious composite. The careful tailoring of the fibre, matrix, and their interface results in a crack-bridging mechanism that triggers a strain-hardening response beyond the first crack up to the ultimate tensile strength of the material. This strain-hardening regime is characterised by multiple diffused cracking with widths usually no more than 100 µm. The strain corresponding to this peak stress determines the composite's strain-hardening capacity. HCP has been demonstrated to be significantly effective in enhancing flexural strengthening, shear strengthening, and increasing the energy dissipation capacity of RC structures (Esmaeeli, 2016; Esmaeeli & Barros, 2015; Esmaeeli & He, 2021). Nonetheless, due to its prefabricated nature, the application of HCP is predominantly limited to flat substrates.

Textile Reinforced Mortars (TRMs) offer an alternative strengthening solution and present a promising material for producing thin prefabricated structural components (De Risi et al., 2020; Koutas et al., 2019; Kulas & Solidian, 2016; Lepenies et al., 2008). TRMs comprise an inorganic matrix – often a cementitious composite – reinforced with a textile grid. Compared to FRP systems, TRMs perform better at elevated temperatures, exhibit superior compatibility with masonry and concrete substrates, and are generally more cost-effective. However, the brittleness of their matrix reduces their effectiveness in enhancing the ductility of strengthened structures and results in large crack widths under service loads. To improve the tensile strength, ductility, and crack control of TRMs, researchers

have explored replacing their brittle matrix with SHCC (Barhum & Mechtcherine, 2013; Gong et al., 2020; Hinzen & Brameshuber, 2009; Li et al., 2019; Orosz et al., 2013; Zheng & Wang, 2016).

The studies were primarily focused on combining various types of SHCCs and textile reinforcement grids, resulting in composites commonly referred to as TR-SHCC. The SHCCs varied in matrix composition, type, and content of short fibres such as carbon, glass, Polyvinyl Alcohol (PVA), Polyethylene (PE), and as-spun PBO. The textile grids were fabricated from glass, carbon, or basalt fibres and adopted with various configurations and volumetric ratios. The outcome of these investigations highlighted that optimised combinations of SHCCs and textile grids result in considerably superior tensile strength, ductility, post-peak behaviour and crack width control compared to those of TRM counterparts. However, despite noteworthy improvements in other mechanical properties, the strain-hardening capacity of most TR-SHCCs developed so far remains limited, often as low as 1%, which could potentially be attributed to inadequate fabric-to-SHCC bonding, stiffness incompatibility, or a combination of both.

The mentioned observation of the low strain-hardening capacity in the TR-SHCCs developed so far serves as the primary motivation for the present study. The objective of this study is to evaluate the effectiveness of the PVA textile grid in creating a TR-SHCC with not only high tensile strength and ductility but also a significant strain-hardening capacity and crack width control ability. PVA, as a hydrophilic fibre, possesses two promising characteristics that can address the aforementioned limitation: a strong chemical bond with the cementitious matrix and a modulus of elasticity that closely aligns with SHCCs.

EXPERIMENTAL PROGRAMME

Material Properties

The textile reinforcement used in this study, commercially known as PVA-Mesh VK1102 and depicted in Figure 1, is a balanced biaxial mesh comprising high-tenacity PVA filaments with a diameter of 14 µm and a linear density of 2 dtex. The textile is manufactured by sandwiching two warp yarns between two weft yarns, each consisting of 1000 PVA filaments, and bonding them with acrylic resin. The mesh opening measures 7 mm × 7 mm and the yarns have a thickness of 0.2 mm. According to the VK1102 supplier, the textile exhibits a tensile strength of 1200 N per 50 mm width and a rupture strain of 8% in both the warp and weft directions.

The SHCC mixture comprised cement type I 42.5R, fly ash, micro silica sand (maximum particle size: 200 µm), chemical admixtures, and short PVA fibres, which were mixed according to the proportion in Table 1. The PVA fibres with commercial brand RECs15×8 had a length of 8 mm and a diameter of 40 µm. According to the supplier, these fibres possess a modulus of elasticity of 40 GPa, a tensile strength of 1600 MPa, and a density of 1300 kg/m³.

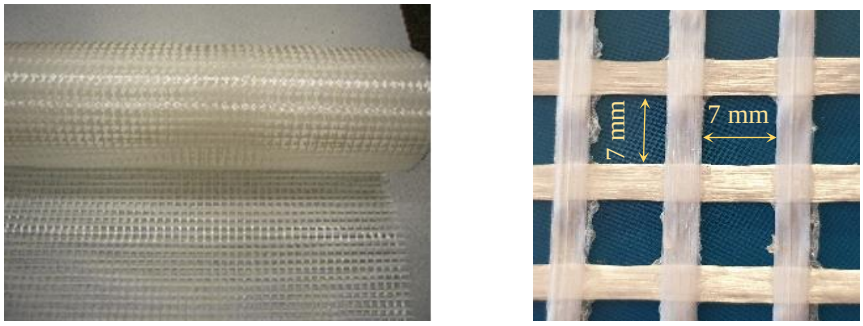

Figure 1: Details of PVA-Mesh VK1102

Table 1: Mix proportion of SHCC (1 m^3)

Cement (kg)	Fly ash (kg)	Micro silica sand (kg)	Limestone powder (kg)	Water (kg)	Chemical admixtures (kg)	PVA fibre (kg)
460	920	160	160	160	146	26

Details and preparation of the specimens

PVA TR-SHCC specimens with five different reinforcement configurations were prepared, and their mechanical behaviour was characterised through direct tensile testing. Two specimens of each configuration were prepared and tested. The main study parameters were the positioning (concentrated *vs* distributed) and the number of textile layers. As illustrated in Figure 2 and detailed in Table 2, specimens **1DL** and **2SL** both featured two layers of textile, but in the former, both layers were placed in the mid-depth of the specimens (one Double-Layer). In the latter, two Single-Layer textiles were positioned at a centre-to-centre distance of 4 mm. Specimens designated as **1TL** consisted of three layers of textile concentrated at mid-depth (one Triple-Layer). Specimens **2DL** and **3DL** comprised two and three double-layer textiles placed at a centre-to-centre distance of 4 mm and 3 mm, respectively.

The specimens were cast in dog-bone shape moulds, utilising the laminating technique. Figure 3a and b show the details of the moulds, consisting of top panels (each 3- or 4-mm thick) and a base plate. This configuration allowed for casting specimens with a nominal thickness of 12 mm, accommodating up to three layers of textile reinforcement. The central part of the moulds maintained a constant width of 50 mm across a length of 160 mm.

The PVA textile strips were cut to a width of 50 mm in the weft direction, comprising five double warp yarns (each weft or warp bundle of fibres of the textile has 2×2000 dtex). The warp yarns of the textile strips were aligned with the longitudinal axis of the moulds.

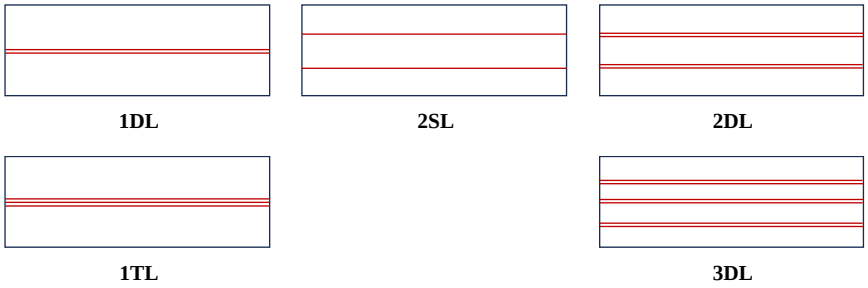

Figure 2: Configuration of PVA textiles of TR-SHCC specimens (cross-section view; 12-mm thick)

Table 2: Details of the specimens

Specimen	Configuration of PVA textile grids	Total number of PVA textile grids	Nominal thickness of each SHCC layer (mm)
SHCC	-	0	12
2SL	2 single layers	2	4
1DL	1 double-layer	2	6
1TL	1 triple-layer	3	6
2DL	2 double-layer	4	4
3DL	3 double-layer	6	3

As shown in Figure 3c, the SHCC was initially cast to the required thickness for each specimen, after which the textile was placed and fixed to the ends of the mould. This procedure was repeated for the specified number of textile layers until the outermost SHCC layer was cast and levelled.

Additionally, two bare SHCC dog-bone specimens were made and tested. The SHCC specimens were cast in moulds similar to those used for producing TR-SHCC specimens but with a shorter length, 80 mm of the central part with constant cross-section.

The fresh specimens were initially cured in a climate-controlled room for 24 hours before demoulding. They were then wrapped in saturated fabric and sealed for curing at 60°C over a 72-hour period. Following this curing cycle, specimens were left unsealed in room environment for an additional 24-hour period before testing.

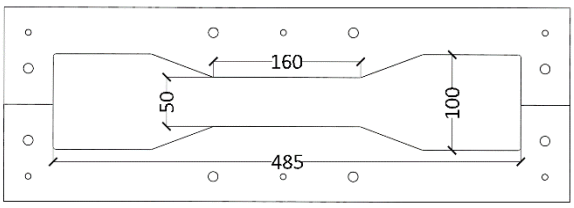

((a)

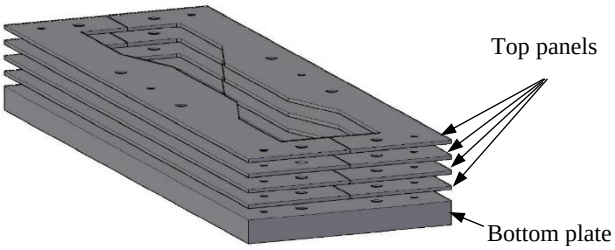

(b)

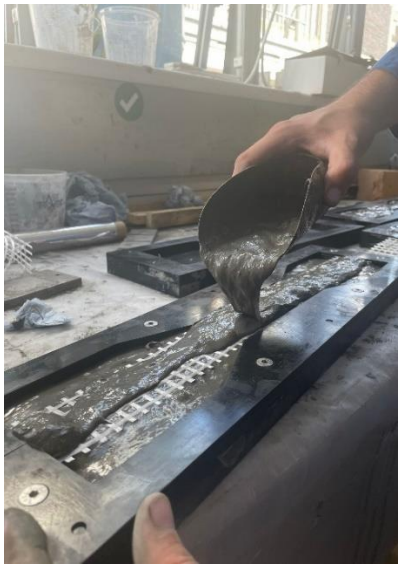

(c)

Figure 3: Details of mould and casting TR-SHCC specimens: (a) dimensions of mould, (b) layered configuration of mould, and (c) casting specimens according to the laminating technique.

Test setup

As demonstrated in Figure 4, the tensile tests were conducted using an Instron material testing machine fitted with a 50 kN load cell, employing a constant cross-head displacement rate of 0.5 mm/min. The top and bottom fixtures were aligned before testing. To measure average elongation, two Linear Vertical Displacement Transducers (LVDTs) were used at a gauge length of 160 mm for TR-SHCC specimens and 80 mm for SHCC specimens. Additionally, a speckle pattern was applied to the specimens' front face to facilitate the 3D Digital Image Correlation (DIC) technique.

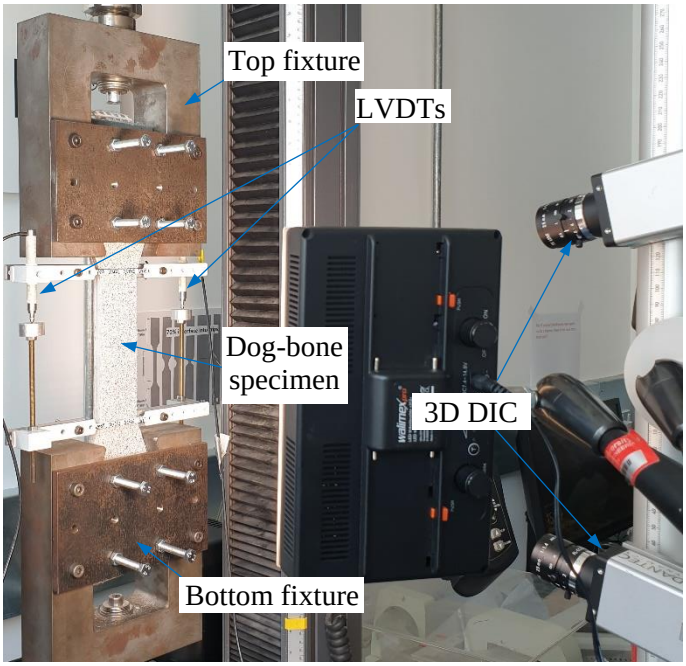

Figure 4: Tensile test setup and instrumentation

RESULTS AND DISCUSSIONS

All tested specimens exhibited diffused fine cracking along and beyond the gauge length. The crack pattern within the gauge length at the end of the test is shown in Figure 5 for one specimen in each group. All TR-SHCC specimens failed by rupture of the PVA grid. Except for specimens 1TL-1, 2DL-2, and both 3DL specimens, failure occurred within the gauge length.

Figure 5: Crack pattern within the 160 mm gauge length (after the failure of the specimens)

The tensile stress-strain curves of the tested specimens are shown in Figure 6. The key results derived from the analysis of these curves - first crack strength, ultimate tensile strength, and strain-hardening capacity - are detailed in Table 3 and compared in Figure 7. The stress is calculated by dividing the load by the cross-section area within the gauge length. The snap back in Figure 6 after the peak stress of specimens 1TL-1, 2DL-2 and both 3DL specimens is attributed to the rupture of the textile reinforcement out of the gauge length.

The test results clearly demonstrate that incorporating the PVA textile grid significantly enhances the ultimate tensile strength and strain-hardening capacity of SHCC. However, the degree of improvement depends on the number and configuration of the textile grids. This observation holds for the first cracking strength, except for 1TL.

A comparison between the tensile behaviour of 2SL and 1DL specimens (Figure 7a) - both with two layers of textile but one with a distributed and the other with a concentrated configuration - reveals that a double-layer textile reinforcement is more efficient in increasing the strain-hardening capacity of the composite, albeit slightly less effective in improving the first cracking strength and ultimate tensile strength. By comparing 1DL and 1TL (Figure 7a), it becomes apparent that not only does a triple-layer fail to improve the ultimate tensile strength and strain-hardening capacity notably, but it also adversely affects the first cracking strength. These results indicate that a double-layer VK1102 PVA textile can develop a sufficient bond with the cementitious matrix, making it a suitable configuration for thin TR-SHCCs containing a large number of textile layers, such as specimens 2DL and 3DL in this study, which incorporate a total of 4 and 6 layers of PVA textile grids, respectively.

As shown in Figure 7b and detailed in Table 3, increasing the number of double-layer textile grids from one to three (specimens 1DL, 2DL, and 3DL) has resulted in a nearly linear but considerable increase in both the ultimate tensile strength and strain-hardening capacity of the TR-SHCC, with the rate of increase in the ultimate tensile strength being slightly higher. For instance, the tensile strength and strain-hardening capacity of 3DL were improved by approximately 74% and 56%, respectively, when compared to 1DL. The first cracking strength has also improved, although the improvement beyond two double-layer textiles was marginal (18% for 3DL versus 15.2% for 2DL compared to 1DL).

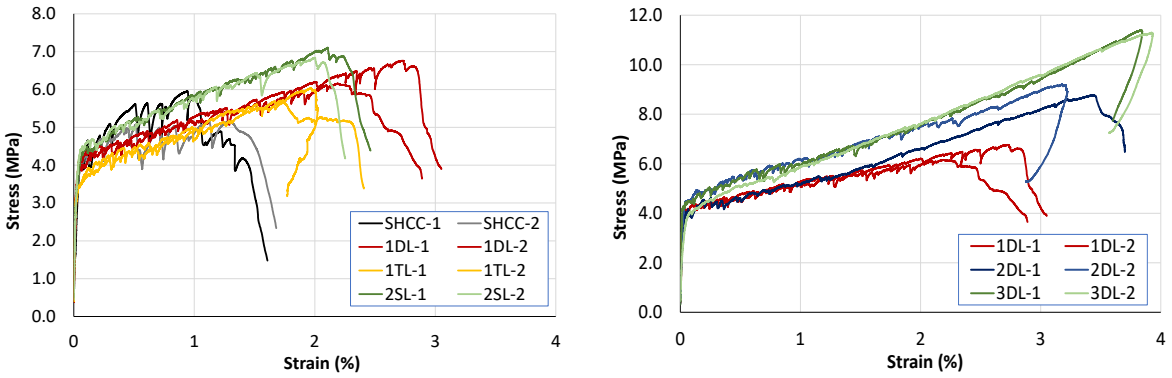

(a) (b)

Figure 6: Tensile stress-strain curves of the tested specimens

Table 3: Key results of tensile tests

Specimen	First Crack Strength Avg. (MPa)	Ultimate Tensile Strength Avg. (MPa)	Strain Hardening Capacity Avg. (%)
SHCC	3.0	5.6	1.0
2SL	3.5 (15.0%) *	7.0 (25.5%)	2.1 (110.0%)
1DL	3.3 (8.3%)	6.5 (16.2%)	2.5 (150.0%)
1TL	2.5 (-17.1%)	5.8 (5.0%)	1.8 (80.0%)
2DL	3.8 (27.2%)	9.0 (6.7%)	3.3 (220.0%)
3DL	3.9 (30.0%)	11.3 (104.1%)	3.9 (290.0%)

* Values between brackets indicate percentage change with reference to SHCC

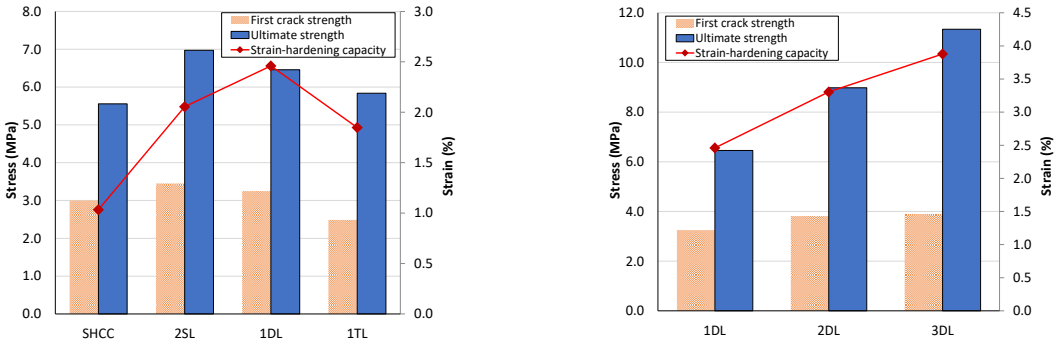

(a) (b)

Figure 7: Comparison of the key results of the tensile behaviour of the tested specimens

Figure 8 represents the evolution of the crack pattern and the average crack width within a 150 mm gauge length at the central part of specimen 3DL-1 (a similar performance was observed in specimen 3DL-2). The average crack width is determined by dividing the overall axial deformation by the number of cracks. Notably, at a strain of 4.0%, where the textile grid is on the verge of rupture, the maximum average crack width remains below 150 µm. This is a promising outcome for applications of TR-SHCC in corrosive environments, such as the repair and strengthening of marine structures.

Upon observing the crack pattern, it becomes evident that the number of cracks increases until a significant strain hardening of 3%. Beyond this point, the crack pattern stabilises, and the average crack width exhibits a linear increase, reaching 144 µm at 4% strain hardening. This phenomenon highlights the excellent synergy between the short and the continuous PVA fibres in effectively controlling crack width as the tensile strength of the TR-SHCC increases.

Figure 9 compares the evolution of the average crack width in specimens 1DL, 2DL, and 3DL. Interestingly, the two double-layer textile configuration (2DL specimens) not only demonstrated superior crack width control compared to the one double-layer configuration (1DL specimens) but also

outperformed the three double-layer configuration (3DL specimens). This finding suggests the existence of a relationship between the volumetric ratio of the PVA textile grid and the thickness of the surrounding SHCC layers, which governs the crack width. This relationship can be optimised to maximise the beneficial combination of the PVA-SHCC and the PVA textile grid.

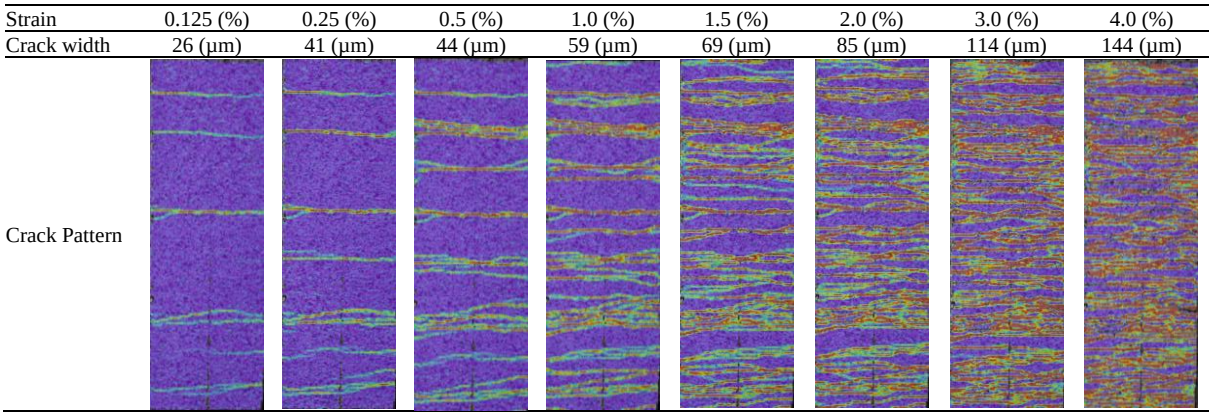

Figure 8: Evolution of the crack pattern and average crack width in specimen 3DL-1 obtained from the DIC analysis within a field of view measuring 150mm × 100mm at the central region of the specimen.

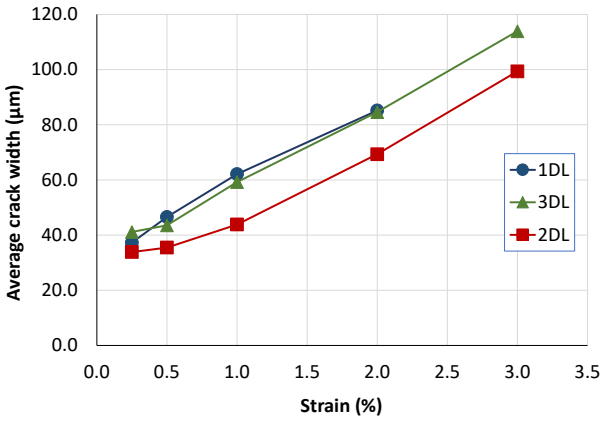

Figure 9: Comparison of the average crack width of double-layer textile specimens

CONCLUSIONS

In recent years several researchers attempted to enhance the tensile strength, ductility, strain-hardening capacity, and crack control feature of TRMs by replacing their brittle matrix with a class of ductile fibrous mortar known as Strain Hardening Cementitious Composites (SHCCs). The resultant composite is often referred to as TR-SHCC. However, despite noteworthy improvements in other mechanical properties, the strain-hardening capacity of most TR-SHCCs remained as low as 1%, which could potentially be attributed to inadequate fabric-to-SHCC bonding, stiffness incompatibility, or a combination of both.

This study aimed at mitigating these shortcomings by evaluating the combination of VK1102 biaxial Polyvinyl Alcohol (PVA) textile grid with PVA-SHCC. The hydrophilic feature of the PVA textile grid and its modulus of elasticity, closely aligned with that of PVA-SHCC, were the primary motives for this combination. The hydrophilic nature of the PVA textile grid fosters a strong chemical bond with the cementitious matrix. Coupled with a modulus of elasticity that aligns closely with that of PVA-SHCC, it enhances the composite action. This, in turn, promotes efficient stress redistribution among the TR-SHCC components: the cementitious matrix, the short PVA fibres, and the PVA textile grid, thereby leading to a higher tensile strength, strain-hardening capacity, ductility and improved control over crack width.

The proposed combination was evaluated through tensile testing of PVA TR-SHCCs across five distinct configurations, with their results compared against each other and the baseline SHCC. The testing results demonstrated clearly that the integration of the PVA textile grid markedly enhances the tensile strength and strain-hardening capacity of the SHCC. The extent of this enhancement is dependent on the number and configuration of the textile grid. Notably, a double-layer PVA textile configuration was found to be more effective in enhancing the strain-hardening capacity of the composite compared to a configuration with two single layers, despite being marginally less effective in improving the first cracking and the ultimate tensile strengths. Conversely, a triple-layer textile configuration decreased the first cracking strength and proved less effective in improving the ultimate tensile strength and strain-hardening capacity. Therefore, it is considered unsuitable for fabricating TR-SHCCs containing multiple layers of the textile grid.

The TR-SHCC with three double-layer PVA textiles (3DL), having a first cracking strength of 3.9 MPa, an ultimate tensile strength of 11.3 MPa, and a strain-hardening capacity of about 4%, exhibited improvements of 30%, 104%, and 290%, respectively, compared to those of the bare SHCC. Notably, the average crack width of the 3DL TR-SHCC at the ultimate tensile strength remained below 150 μm, which is a promising feature for applications in corrosive environments with dynamic actions, such as repairing and strengthening marine structures.

Among the tested configurations, the two double-layer textiles (2DL) demonstrated superior crack width control. This finding highlights the potential for achieving an optimal relationship between the PVA textile grid's volumetric ratio and the SHCC layers' thickness to maximise the benefits of combining the PVA textile grid with PVA-SHCC.

ACKNOWLEDGMENT
The authors would like to acknowledge Kuraray Co., Ltd. for supplying the PVA materials.

CONFLICT OF INTEREST
The authors declare that they have no conflicts of interest associated with the work presented in this paper.

DATA AVAILABILITY
Data on which this paper is based is available from the authors upon reasonable request.

REFERENCES

Barhum, R., & Mechtcherine, V. (2013). Influence of short dispersed and short integral glass fibres on the mechanical behaviour of textile-reinforced concrete. *Materials and Structures/Materiaux et Constructions*, *46*(4), 557–572. https://doi.org/10.1617/s11527-012-9913-3

De Risi, M. T., Furtado, A., Rodrigues, H., Melo, J., Verderame, G. M., António, A., Varum, H., & Manfredi, G. (2020). Experimental analysis of strengthening solutions for the out-of-plane collapse of masonry infills in RC structures through textile reinforced mortars. *Engineering Structures*, *207*(November 2019), 110203. https://doi.org/10.1016/j.engstruct.2020.110203

Esmaeeli, E. (2015). Development of Hybrid Composite Plate (HCP) for the Strengthening and Repair of RC Structures [University of Minho]. In *Civil Eng. Dept.* https://doi.org/http://hdl.handle.net/1822/40465

Esmaeeli, E. (2016). A review on development and applications of Hybrid Composite Plate (HCP): a robust retrofitting solution for RC members. *Proceedings of the 8th International Conference on Fibre-Reinforced Polymer (FRP) Composites in Civil Engineering, CICE 2016*.

Esmaeeli, E., & Barros, J. A. O. (2015). Flexural strengthening of RC beams using Hybrid Composite Plate (HCP): Experimental and analytical study. *Composites Part B: Engineering*, *79*, 604–620. https://doi.org/10.1016/j.compositesb.2015.05.003

Esmaeeli, E., Barros, J., & Sena-Cruz, J. (2013). *Painel compósito híbrido para o reforço de estruturas de betão existentes e respetivo método de produção e de aplicação.* (Patent No. 107111). Instituto Nacional da Propriedade Industrial (INPI).

Esmaeeli, E., & He, Y. (2021). Cast-in-situ vs prefabricated solution based on NSM-CFRP reinforced SHCC for seismic retrofitting of severely damaged substandard RC beam-column joints. *Journal of Building Engineering*, *43*(July), 103132. https://doi.org/10.1016/j.jobe.2021.103132

Gong, T., Ahmed, A. H., Curosu, I., & Mechtcherine, V. (2020). Tensile behavior of hybrid fiber reinforced composites made of strain-hardening cement-based composites (SHCC) and carbon textile. *Construction and Building Materials*, *262*, 120913. https://doi.org/10.1016/j.conbuildmat.2020.120913

Hinzen, M., & Brameshuber, W. (2009). Improvement of Serviceability and Strength of Textile Reinforced Concrete by using Short Fibres. *4th Colloquium on Textile Reinforced Structures (CTRS4), part I*, 261–272.

Koutas, L. N., Tetta, Z., Bournas, D. A., & Triantafillou, T. C. (2019). Strengthening of Concrete Structures with Textile Reinforced Mortars: State-of-the-Art Review. *Journal of Composites for Construction*, *23*(1), 1–20. https://doi.org/10.1061/(asce)cc.1943-5614.0000882

Kulas, C., & Solidian. (2016). *Actual applications and potential of textile-reinforced concrete*.

Lepenies, I. G., Richter, M., & Zastrau, B. W. (2008). A Multi-Scale Analysis of Textile Reinforced Concrete Structures. *PAMM*, *8*(1), 10553–10554. https://doi.org/https://doi.org/10.1002/pamm.200810553

Li, B., Xiong, H., Jiang, J., & Dou, X. (2019). Tensile behavior of basalt textile grid reinforced Engineering Cementitious Composite. *Composites Part B: Engineering*, *156*(May 2018), 185–200. https://doi.org/10.1016/j.compositesb.2018.08.059

Orosz, K., Blanksvärd, T., Täljsten, B., & Fischer, G. (2013). Crack development and deformation behaviour of CFRP-reinforced mortars. *Nordic Concrete Research*, *48*(1), 49–69. https://www.diva-portal.org/smash/record.jsf?pid=diva2:988064

Zheng, Y., & Wang, W. (2016). *Tensile behaviour of FRP grid strengtheneing ECC composite under a uniaxial loading*. *2*, 529–535. https://doi.org/10.14264/uql.2016.1149